# MOTIFS, ALGEBRAIC CONNECTIVITY AND COMPUTATIONAL PERFORMANCE OF TWO DATA-BASED CORTICAL CIRCUIT TEMPLATES

*Heinz Koeppl*[1] *and Stefan Haeusler*[2]

[1]School of Computer and Communication Sciences, EPFL, Switzerland
[2]Institute for Theoretical Computer Science, Graz University of Technology, Austria

## ABSTRACT

Based on extensive experimental work two templates for the laminae-specific connectivity pattern of cortical microcircuits have recently been published. We examine their structural and computational properties and attempt to correlate those properties. To characterize structure or circuit topology we consider the distribution of network motifs as well the algebraic connectivity of the network. In order to understand the computational properties of these two templates, we have generated computer models of them, consisting of Hodgkin-Huxley point neurons with conductance based synapses that have a biologically realistic short-term plasticity. The performance is assessed using nine generic computational tasks that require accumulation and merging of information contained in two afferent spike inputs.

## 1. INTRODUCTION

Neurobiological studies have shown that cortical circuits have a distinctive modular and laminar structure, with stereotypical connections between neurons that are repeated throughout many cortical areas (see [1] and the references therein). It has been conjectured that these stereotypical canonical microcircuits are not merely an artifact of the specific mapping of afferent and efferent cortical pathways or other anatomical constraints like evolutionary processes or development, but are also advantageous for generic computational operations that are carried out throughout the neocortex.

Over the past years detailed statistical data became available that are based on two different experimental methods became available: dual intracellular recordings in vitro and cell morphology. The first dataset assembled by [2] was estimated from 998 paired intracellular recordings with sharp electrodes in slices of somatosensory, motor and visual areas of adult rats and adult cats. It specifies connection probabilities and connection strengths of effectively established synaptic connections between excitatory and inhibitory neocortical neurons, to which we will refer as functional connectivity in this paper. The second dataset assembled by [3] was predicted from bouton and target densities in cat primary visual cortex estimated from three-dimensional cell reconstructions. This dataset does not specify the distribution of functional connections, but rather represents potential synaptic connectivity.

We investigate these two cortical microcircuit templates with regard to local and global structural properties. In particular we are interested to establish a link between their structural and functional properties. In order to evaluate the computational properties of microcircuit templates we carried out computer simulations of detailed cortical microcircuit models.

Similar to [4], our analysis is based on the assumption that stereotypical cortical microcircuits have some "universal" computational capabilities, and can support quite different computations in different cortical areas. Consequently we concentrate on generic information processing capabilities that are likely to be needed for many concrete computational tasks: to accumulate, hold and fuse information contained in Poisson input spike trains from two different sources (modeling thalamic or cortical feedforward input that arrives primarily in layer 4, and lateral or top-down input that arrives primarily in layers 2/3).

Here we investigate possible dependencies of the computational performance of two cortical microcircuit templates of [2] and [3] on local as well as global characteristic of the circuit topology. In particular we consider the motif distribution and the algebraic connectivity, respectively. In order assess the significance of these graph characteristics of the two data-based microcircuit templates we compare them with those of random control circuits.

## 2. CIRCUITS AND COMPUTATIONAL TASKS

The cortical microcircuit model according to the microcircuit template assembled by [2] consisted of 600 neurons located in layers 2/3, layer 4, and layer 5. The microcircuit model according to the microcircuit template assembled by [3] consisted of the same number of neurons but includes an additional layer 6. Each layer consisted of a population of excitatory neurons (E) and inhibitory neurons (I) with a ratio of 4:1. The synaptic connection probabilities of both models were rescaled to achieve on average the same number of 42000 synaptic connections. Because the cortical microcircuit template of [3] provides no strengths of synaptic connections the corresponding values were adopted according to the template of [2]. Neurons were modeled as conductance based single compartment Hodgkin-Huxley point neurons. Background input currents that were injected into each neuron, reflecting input currents from a large number of more distal neurons,

modeled as a one-variable stochastic process similar to an Ornstein-Uhlenbeck process. The short term synaptic dynamics (paired pulse depression and facilitation) was modeled according to [5], with synaptic parameters chosen to fit data from microcircuits in rat somatosensory cortex. Two afferent input streams were injected into the circuit. The first input stream (representing thalamic input) was injected mainly into layer 4, whereas the second afferent input stream was injected into neurons in layers 2/3.

We modeled hypothetical projection neurons in layers 2/3 and layer 5 as linear neurons. The weights of synaptic connections from the presynaptic neurons to the readout neuron were optimized for specific tasks. The information processing tasks comprised spike pattern classification, i.e. classification of spike patterns in either of the two afferent input streams, as well as real-time computations on the firing rates of both input streams (tasks 1-5). For information processing tasks with spike patterns readout neurons were trained to classify which of the two spike templates fixed for input 1 (input 2) was injected during the last time interval $[t - 30\ ms, t\ ms]$, denoted as task $\mathrm{tcl}_1(t)$ ($\mathrm{tcl}_2(t)$), or during the preceding time interval $[t - 60\ ms, t - 30\ ms]$, denoted as task $\mathrm{tcl}_1(t - \Delta t)$ ($\mathrm{tcl}_2(t - \Delta t)$). Note that the latter task may be viewed as a memory task (with distractors). Nonlinear fusion of information from both input streams was tested by training readouts to output the exclusive-or (XOR) of the two bits that represent the labels of the two templates from which the most recent spike patterns in the two input streams had been generated (task 5). This computation involves a nonlinear "binding" operation on spike patterns. In addition we analyzed nonlinear computations on time-varying firing rates of input stream 1, $r_1(t)$, and input stream 2, $r_2(t)$. $(.)_{NL}$ denotes computations on the purely nonlinear components of the specified tasks (tasks 6-9). For further details see [4].

Control circuits have the same components and the same global statistics of neurons and synaptic connections. Amorphous circuits were generated from data-based circuits by randomly rewiring recurrent synaptic connections whereas no synaptic connection was allowed to occur more than once. The rewiring was carried out under the constraint that the pre- and postsynaptic neuron type (i.e. E or I) of each synaptic connection stays the same. Degree-controlled circuits preserve the degree distributions of neurons in all layers but otherwise lack a laminae-specific connectivity pattern. Degree-controlled circuits were constructed from data-based circuits by randomly exchanging the target neurons of pairs of recurrent synaptic connections that emerge from the same neuron, and have neurons of the same type (i.e. E or I) as target. For the circuits in Fig. 3 and Fig. 4 indicated as EE, IE, EI and II the rewiring was carried out under the constraint that only synaptic connections with postsynaptic neurons of the type indicated by the first letter (i.e. E or I) and presynaptic neurons of the type indicated by the second letter (i.e. E or I) were scrambled.

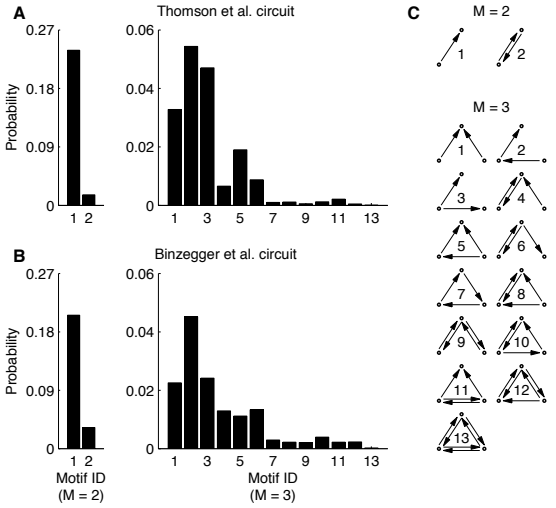


Figure 1. Two-node and three-node motif distributions for the Thomson et al. (A) and Binzegger et al. (B) cortical microcircuit template; (C) enumeration of all possible two-nodes and three-node motifs.

## 3. MOTIFS

Motifs are stereotypical connectivity pattern on a local scale. They commonly are taken to be all possible connectivity patterns between three or four nodes. In realistic networks particular motifs appeared to be overrepresented [6]. Attempts have been made to attribute them particular signal processing functions. For instance a three-node coherent feedforward motifs is considered a sign-sensitive persistence filter [6] in transcriptional networks. Here we investigate the two-node and three-node motif distributions for the two considered microcircuit templates. In Fig. 1 their respective motif distribution is shown. The significance of these motif distributions with respect to amorphous variants is assessed using the Z-score, i.e., the difference in motif count between the data-based microcircuit and its amorphous variant normalized by the standard deviation of the motif count for the amorphous circuit. The Z-score for the two data-based circuits is shown in Fig. 2.

## 4. ALGEBRAIC CONNECTIVITY

Algebraic connectivity was introduce by Fiedler [7] and was shown to be related to other important graph characteristics such as the diameter or the classical connectivity of a graph. Algebraic connectivity also appeared to be central for the synchronizability of an ensemble of dynamical systems coupled over a network. The higher the algebraic connectivity, the lower the required coupling strengths between the systems in order to achieve complete synchronization of the ensemble [8]. These finding represents the motivation of the current work to investigate the relation of this graph measure to the computational performance. For undirected graphs algebraic connectivity is determined by the second largest eigenvalue of the Laplacian matrix of the graph [7]. Several extensions

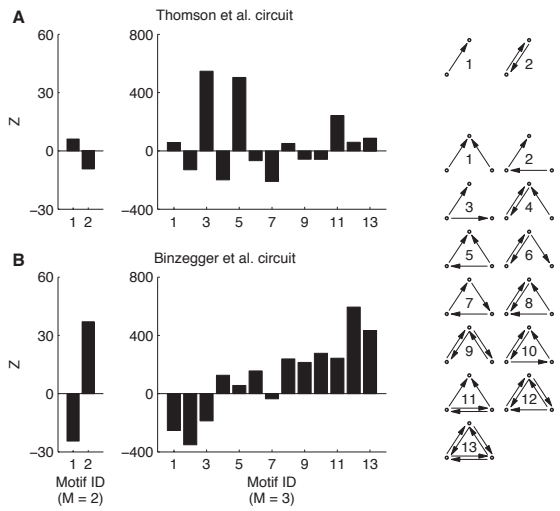


Figure 2. Z-score (defined as the difference in the average motif count for the specified circuits and corresponding amorphous circuits measured in units of the standard deviation of the motif count for amorphous circuits) for Thomson et al. circuit (A) and Binzegger et al. circuit (B).

to directed graphs exists, two of which will be considered in the sequel. We will refer to them as connectivity according to C. W. Wu or F. Chung indicating where they were proposed [8, 9]. Following [9] a random walk on a directed graph can be defined by denoting

$$P_{ij} = \frac{A_{ij}}{d_i} \tag{1}$$

whereas $A_{ij}$ denotes an element of the adjacency matrix of the graph and $d_i = \sum_j A_{ij}$ is the out-degree of node $i$. The matrix $\mathbf{P}$ is a valid transition matrix of a discrete-time Markov chain, i.e., its contains only non-negative elements and the rows sum up to one

$$\mathbf{P}\mathbf{e} = \mathbf{e}$$

with the $N$-dimensional unit vector $\mathbf{e} = (1, \ldots, 1)^T$. Strong connectedness of a directed graph means that there exits a directed path from every node to every other node. If the graph is strongly connected according to the Frobenius-Perron theorem the matrix $\mathbf{P}$ has a simple eigenvalue of one and the corresponding left eigenvector is the stationary distribution of the Markov chain

$$\boldsymbol{\phi}\mathbf{P} = \boldsymbol{\phi}$$

and sometimes called the Perron vector. The Laplacian of a directed graph can then be defined according to [9] as

$$\mathbf{L} = \mathbf{I} - \frac{\boldsymbol{\Phi}^{1/2}\mathbf{P}\boldsymbol{\Phi}^{-1/2} + \boldsymbol{\Phi}^{-1/2}\mathbf{P}^T\boldsymbol{\Phi}^{1/2}}{2} \tag{2}$$

with $\boldsymbol{\Phi} = \mathrm{diag}(\boldsymbol{\phi})$. We denote the second smallest eigenvalue of $\mathbf{L}$ as the connectivity according to F. Chung.

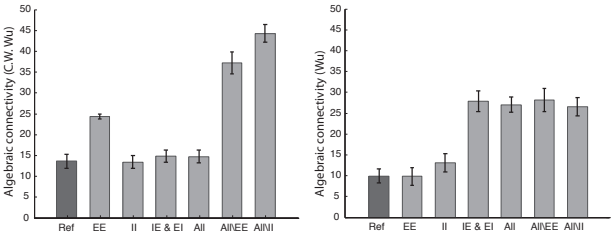


Figure 3. Mean and standard deviation of algebraic connectivity according to C. W. Wu [8] for 100 random realizations of the Thomson et al. circuit (left) and Binzegger et al. circuit (right) and six amorphous variants thereof.

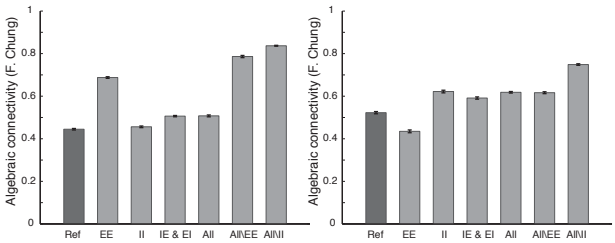


Figure 4. Mean and standard deviation of algebraic connectivity according to F. Chung [9] for 100 random realizations of the Thomson et al. circuit (left) and Binzegger et al. circuit (right) and six amorphous variants thereof.

Equation (2) is a normalized version of the *combinatorial* Laplacian [9] $\tilde{\mathbf{L}} = \boldsymbol{\Phi}^{1/2}\mathbf{L}\boldsymbol{\Phi}^{1/2}$

$$\tilde{\mathbf{L}} = \boldsymbol{\Phi} - \frac{\boldsymbol{\Phi}\mathbf{P} + \mathbf{P}^T\boldsymbol{\Phi}}{2}$$

An alternative definition of the Laplacian for directed graph, that is analog to that of an undirected graph involves the outdegrees of nodes [8]

$$\hat{\mathbf{L}} = \mathrm{diag}(\mathbf{d}) - \mathbf{A}.$$

The connectivity according to C. W. Wu is then the smallest eigenvalue of the matrix $\frac{1}{2}\mathbf{Q}^T(\hat{\mathbf{L}} + \hat{\mathbf{L}}^T)\mathbf{Q}$, where $\mathbf{Q}$ is a $N \times (N-1)$ matrix with orthonormal columns that are orthogonal to the unit vector $\mathbf{e}$, where $N$ denotes the number of nodes.

The algebraic connectivity according to C. W. Wu and F. Chung for both considered data-based circuits and their amorphous variants are shown in Fig. 3 and Fig. 4, respectively.

## 5. RESULTS AND DISCUSSION

The motif distributions of Thomson et al. circuits and Binzegger et al. circuits differ significantly. The connectivity patterns of Thomson et al. circuits show a distinctive motif distribution with over-represented three-node motifs 3, 5, and 11 and lacking motifs 2, 4, and 7 when compared to amorphous networks (see Fig. 2). In contrast for Binzegger et al. circuits highly connected three-node motifs are over-represented, whereas motifs consisting of only two links occur less frequent compared to

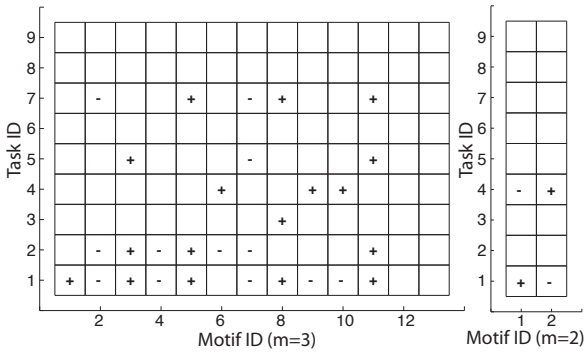


Figure 5. Significant (Spearman $\rho < 0.05$ or Pearson $p < 0.05$) positive or negative correlation between three-motif (left) and two-motif counts (right) and computational performance for nine different task for the Thomson et al. circuit; not significant correlation are indicated by empty boxes.

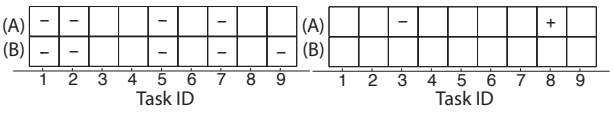


Figure 6. Significant (Spearman $\rho < 0.05$ or Pearson $p < 0.05$) positive or negative correlation between algebraic connectivity according to C. W. Wu (A) and C. Chung (B) and computational performance for the Thomson et al. circuit (left) and the Binzegger et al. circuit (right); not significant correlation are indicated by empty boxes.

corresponding amorphous networks. We further showed for Thomson et al. circuits that the frequency of specific three-node motifs is correlated with performance for the chosen set of 9 information processing tasks. It turned out that the absolute difference in motif probability between the databased microcircuit and its amorphous variant is positively correlated with the computational performance of various tasks, in particular for the 6 characteristic motifs specified above (see Fig. 5). Therefore the superior computational performance of Thomson et al. circuits when compared to its amorphous variant can not be attributed to the more or less frequent occurrence of single motifs, but is rather a property of the characteristic motif distribution as a whole. Algebraic connectivity according to F. Chung [9] turned out to be a discriminate measure for the data-based circuit and its various control circuits (see Fig. 4) because of its low variance. The computational performance for Thomson et al. circuit shows a significant negative correlation consistent throughout all tasks (see Fig. 6). This does not hold for the Binzegger et al. circuit. The finding that a higher connectivity of the network deteriorates the computational performance is consistent with the observation that sparse heterogeneous networks support higher computational performance than dense and uniform networks.

## 6. CONCLUSION

We considered two recently published data-based cortical microcircuit templates and compared their local and global structural features in the light of their computational performance for nine generic tasks. For reference we generated a collection of random control circuits that lack the laminae-specific connectivity pattern of the templates but comprise the same number of components. We found that both circuits show distinctive motif distribution compared with their control variants. We found for the Thomson et al. circuit that particular three-node motifs are consistently positively correlated with the computational performance and that the algebraic connectivity is negatively correlated with the performance for specific tasks.

## 7. ACKNOWLEDGMENTS

H.K. acknowledges the support from the Swiss National Science Foundation (SNF), grant 200020-117975/1.

# References

[1] N. Kalisman, G. Silberberg, and H. Markram, "The neocortical microcircuit as a tabula rasa," *Proc Natl Acad Sci*, vol. 102, no. 3, pp. 880–885, 2005.

[2] A. M. Thomson, D. C. West, Y. Wang, and A. P. Bannister, "Synaptic connections and small circuits involving excitatory and inhibitory neurons in layers 2 - 5 of adult rat and cat neocortex: triple intracellular recordings and biocytin labelling in vitro," *Cerebral Cortex*, vol. 12, no. 9, pp. 936–953, 2002.

[3] T. Binzegger, R. J. Douglas, and K. A. Martin, "A quantitative map of the circuit of cat primary visual cortex," *J. Neurosci.*, vol. 24, no. 39, pp. 8441–8453, 2004.

[4] S. Häusler and W. Maass, "A statistical analysis of information processing properties of lamina-specific cortical microcircuit models," *Cerebral Cortex*, vol. 17, no. 1, pp. 149–62, 2007.

[5] H. Markram, Y. Wang, and M. Tsodyks, "Differential signaling via the same axon of neocortical pyramidal neurons," *PNAS*, vol. 95, pp. 5323–5328, 1998.

[6] U. Alon, "Network motifs: theory and experimental approaches," *Nature Genetics Review*, vol. 450, no. 8, pp. 450–461, 2007.

[7] M. Fiedler, "Algebraic connectivity of graphs," *Czechoslovak Mathematical Journal*, vol. 23, no. 98, pp. 298–305, 1973.

[8] C. W. Wu, "Algebraic connectivity of directed graphs," *Linear and Multilinear Algebra*, vol. 53, no. 3, pp. 203–223, 2005.

[9] F. Chung, "The diameter and Laplacian eigenvalues of directed graphs," *Electronic Journal of Combinatorics*, vol. 13, no. 1, pp. 6, 2006.